

# Burner air-fuel ratio monitoring in large pulverised-fuel boilers using advanced sensors: case study of a 660MWe coal-fired power plant.

J. Blondeau<sup>a,b,\*</sup>, L. Rijmenans<sup>c</sup>, J. Annendijck<sup>c</sup>, A. Heyer<sup>d</sup>, E. Martensen<sup>d</sup>, I. Popin<sup>e</sup>, A. Wijittongruang<sup>e</sup>, L. Holub<sup>e</sup>

<sup>a</sup>*Thermo and Fluid dynamics (FLOW), Faculty of Engineering, Vrije Universiteit Brussel (VUB), Pleinlaan 2, 1050 Brussels, Belgium*

<sup>b</sup>*Combustion and robust optimization (BURN), Vrije Universiteit Brussel (VUB) and Universit Libre de Bruxelles (ULB)*

<sup>c</sup>*Laborelec (ENGIE), Rodestraat 125, 1630 Linkebeek, Belgium*

<sup>d</sup>*EUtech Scientific Engineering, Dennewartstrasse 25-27, 52068 Aachen, Germany*

<sup>e</sup>*Gheco-One (ENGIE), Map Ta Phut Industrial Estate, I-5 Road 11, 21150 Rayong, Thailand*

---

## Abstract

In this paper, a novel methodology is proposed for the online monitoring of the air-fuel ratio in large pulverised-fuel boilers at the burner level. Using standard measurements, this parameter can only be estimated, as the fuel distribution between burners is generally missing. The detailed air flow distribution to the burners can also be unknown depending on the available measurements. An accurate control of local and global air-fuel ratios is however crucial in terms of boiler efficiency and  $NO_x$  emissions. It is here proposed to combine two advanced techniques to quantify air and fuel flow rates per burner: microwave probes for fuel particles and smart soft sensors for air. When combined, those measurements allow for the calculation of the local air-fuel ratios. The proposed methodology was successfully applied to the boiler of a 660 MWe coal-fired power plant. While the burner equivalence ratios predicted by the standard equipments were in the range 0.9 – 1.05, it was shown that the actual range was significantly broader (0.65 – 1.25). Looking at the averaged ratios per burner level, it was concluded that the expected values were globally overestimated

---

\*Corresponding author: julien.blondeau@vub.ac.be

compared to the measured values ( $> +14\%$ ). The performed air flow measurements were also used to tune the combustion process by solving hardware and software issues. Oxygen, flue gas flow rate, temperature and  $NO_x$  unbalances at the outlet of the furnace were significantly reduced.

*Keywords:* power plant, coal, air-fuel ratio, coal flow

---

## 1. Introduction

In 2014, the share of electricity produced in the world from coal combustion was 40.8% [1]. While this share will need to be drastically reduced in the coming decades to reach the current  $CO_2$  emission targets, it is nonetheless important to keep on increasing the efficiency of the existing assets worldwide in order to limit their global environmental impact. When possible, the most recent and accurate techniques should be used to control the processes of the coal-fired power plants [2]. A recent report published by the IEA Clean Coal Center emphasises that the use of new equipment available on the market can help the operators to optimise their operation for better performances and less pollution [3].

The release of thermal energy in the combustion chamber is the core process of thermal power plants. Not only the global efficiency of the plant, but also part of the pollutant emissions at the stack, depends greatly on the quality of the combustion process [4]. In large pulverised-fuel boilers (PF-boilers), the main control parameters are the fineness of the fuel particles and the air-fuel distribution in the combustion chambers [5]. An efficient combustion process requires sufficient temperature, sufficient residence time and good mixing between air and fuel. As primary measures can also be applied in the furnace to limit the production of  $NO_x$ , trade-offs between combustion efficiency and limited need for flue gas treatment downstream of the boiler are often to be found [2].

### 1.1. Air-Fuel Ratio

For a given fuel fineness provided by the mills, the Air-Fuel Ratio (AFR) is the key factor to be controlled to optimise the combustion process in terms of efficiency and environmental impact. The AFR is defined as the ratio between the injected flow rate of air  $\dot{m}_a$  and the injected flow rate of fuel  $\dot{m}_f$ :

$$AFR = \frac{\dot{m}_a}{\dot{m}_f} \quad (1)$$

The AFR is closely related to the air-fuel equivalence ratio  $\lambda$ , defined as the ratio between the injected flow rate of air (or oxygen) and the flow rate of air (or oxygen) that is strictly needed to burn the considered amount of fuel. The latter is called stoichiometric.

$$\lambda = \frac{\dot{m}_a}{\dot{m}_{a,stoi}} = \frac{AFR}{AFR_{stoi}} \quad (2)$$

Values of  $\lambda$  lower than 1 define sub-stoichiometric conditions, inevitably leading to the production of  $CO$  and residual unburned carbon in bottom and fly ash streams. Values of  $\lambda$  greater than 1 lead to the presence of excess oxygen in the flue gas. For a good combustion process (high temperature, long residence time, and good mixing), this also tends to reduce the production of  $CO$  and unburned carbon to acceptable levels.

$\lambda$  can be defined for the whole furnace, but also per burner or burner row. Local conditions in the furnace can therefore differ from the global air-fuel balance in terms of stoichiometry.

### 1.2. Air staging

The production of thermal  $NO_x$  in the furnace is greatly reduced when air staging is applied. This primary measure tends to favour reducing atmospheres in the areas of the furnace where the peak temperatures are observed, and also to limit these peak temperatures. Those two factors reduce the concentration of  $NO_x$  at the outlet of the furnace. Locally reducing atmosphere implies that  $\lambda$

is locally smaller than 1. Other primary measures include flue gas recirculation, fuel-staging or water/steam injection [2].

Using air-staged low- $NO_x$  burners, air staging is applied at the level of the flame. A secondary and a tertiary air streams are separated from the primary air carrying the fuel particles, which literally stages the combustion, and produces a reducing atmosphere in the core of the flame, where  $\lambda < 1$ . Air-staged low- $NO_x$  burners can achieved  $NO_x$  reduction in the range 25 – 50%. Other types of low- $NO_x$  burners include fuel-staged or flue-gas recirculation burners [2].

Air-staging can also be applied globally in the furnace. By injecting sub-stoichiometric amount of air in the lowest burner rows, a global reducing atmosphere can be created in a significant volume of the furnace ( $\lambda < 1$ ), while decreasing the peak flame temperature. In order to ensure a complete burn-out of the fuel particles (and therefore limit  $CO$  emissions and unburned carbon in ash), this reduced air flow rate must be compensated by higher  $\lambda$ 's at the level of the highest burner rows, or through specific Over Fire Air injection ports (OFA ports). In modern, large pulverised-fuel boilers, a global  $\lambda$  in the range 1.1 – 1.3 must be reached at the outlet of the boiler. This corresponds to an excess oxygen concentration in the flue gas in the range 2 – 4%. The efficiency of global air-staging on  $NO_x$  reduction is dependent on several operational and design parameters. It is reported that it can achieve between 10 and 70% of  $NO_x$  reduction [2].

The use of low- $NO_x$  burners can also be combined with global-air staging and OFA. In this case, the value of  $\lambda$  reached at the burner level may be lower than 1. When applied, this technique can lead to a  $NO_x$  reduction up to 70% [2].

### 1.3. Combustion efficiency, corrosion and slagging issues

The use of global air-staging for  $NO_x$  emission control has however three main potential drawbacks: decrease of combustion efficiency, boiler wall corrosion and slagging [2, 4]. The creation of a reducing atmosphere in a significant volume of the furnace increases the local concentration of  $CO$  and slows down

the oxidation of the char particles. Even if a sufficient amount of air is globally injected in the furnace ( $\lambda = 1.1 - 1.3$  beyond OFA), the complete oxidation of  $CO$  and char may be hindered by a too short residence time or incomplete mixing of flue gases and air after the OFA. This can result in an increase emissions of  $CO$  and unburned carbon compared to a conventional combustion process. An increased  $CO$  concentration along some parts of the boiler wall can also cause accelerated corrosion, sometimes improperly called ‘ $CO$  corrosion’.  $CO$  itself doesn’t cause corrosion to occur, but reducing conditions favour corrosion by sulfur, chlorine or other corrosive elements [6]. Finally, it is well known that the ash melting temperature of some fuels drastically decreases in reducing conditions [7]. High iron-content coals are particularly concerned, as their ash softening temperature can decrease with 100 to 200°C when they are burned in reducing conditions [8]. Ash deposition on the radiant heat surfaces of the boiler, called slagging, decreases the boiler performances and can also lead to tube damages.

#### 1.4. Monitoring of Air Fuel Ratio

In a typical pulverised-fuel boiler, the global air-fuel ratio can be easily monitored using the total flow rates of fuel and air injected in the boiler. The total fuel flow rate can be computed as the sum of the flow rates measured by the feeders of each mill. The total amount of air is generally measured at the outlet of the primary and secondary air fans using Venturi measurement devices, that are known to be reliable and accurate [9]. The global equivalence ratio  $\lambda$  can also be assessed when the composition of the fuel is known, as the stoichiometric amount of air needed to completely burn each kilogram of fuel can therefore be computed. It should be noted that in practice the fuel moisture content is the parameter subject to the largest uncertainty, as the fuel might have been partially dried or further humidified between the analysis and the injection in the feeders, depending on the handling and the weather conditions.

In order to accurately control the applied air-staging, the additional monitoring of the local AFR and  $\lambda$  per burner (or at least per burner row) is needed

[3]. However, the standard equipments available in power plants do not allow for the direct measurement of these parameters, as the local fuel and air flow rate are generally not available or inaccurate.

110 The fuel particle distributions between burners is generally unknown [3, 5]. Only the total flow rates measured by the mills' feeders are available. The way these flow rates are distributed among the burners fed by a given mill is not measured. The only way to compute a local AFR or  $\lambda$  is to suppose that the fuel distribution between burners is uniform. The return of experience from  
115 onsite, dedicated measurement campaigns shows that the discrepancy between the expected average value and the measured flow rates can easily reach 10–15% [5].

Not all boilers are equipped with air flow rate measurements per burner, not even per row. When they are, velocity measurement techniques (like multiport  
120 Pitot tubes) are generally preferred to obstruction flow meters (like Venturi, nozzle or orifice devices), only considered for total flow measurements at the outlet of the fans. The full calibration of these local measurements is done during the boiler commissioning, by comparison with manual, grid-measurements. Correction factors are applied to account for the imperfect location of the mea-  
125 suring orifices, with values reaching sometimes several tens of percents. During the lifetime of the boiler, the pressure transducers are regularly re-calibrated during maintenance, but rarely the global measurement systems. For these reasons, the local measurements are considered less reliable than the total flow measurements performed at the outlet of the fans by the operators. They are  
130 most of times used to compare burners or to draw conclusions on trends, but rarely for the assessment of AFR's. A large discrepancy between the measured total flow rates and the sum of the local flow rates can be observed, as will be showed in this study.

### *1.5. Advanced monitoring equipments*

135 In this study, advanced equipments have been used to accurately monitor the fuel and air flow rates at the burner level on the boiler of a 660  $MW_e$  coal-

fired PF-boiler. The used equipments are listed in a recent IEA report [3] as part of the most advanced equipments available. An online monitoring of the local AFR's and equivalence ratios  $\lambda$  was therefore achieved. The equipment used to monitor the fuel distribution to the burners is presented in §2.1. The equipment used to monitor the air flow distribution is presented in §2.2.

The objectives of this paper are to:

1. Propose a methodology for the monitoring of local AFR's and equivalence ratios  $\lambda$  in large utility boilers, using advanced commercial equipments;
2. Present the case study of a modern 660  $MW_e$  coal-fired PF-boiler.

## 2. Equipment and methodology

### 2.1. Coal flow distribution to burners: microwave sensors

The standard way to monitor the amount of solid fuel fed into a PF-boiler is to measure the flow rate delivered by the feeders to the mills [10, 2, 5]. There are two main types of feeders: volumetric or gravimetric. The volumetric feeders, illustrated in Fig. 1, maintain a constant speed vs. volume relationship (for a given bed thickness). The gravimetric feeders, illustrated in Fig. 2, constantly weight the conveyed fuel for an automatic control of the mass flow rate [10].

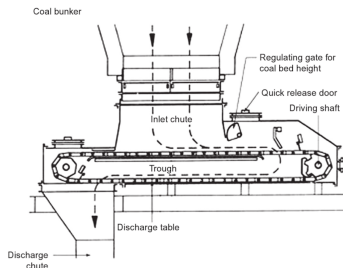


Figure 1: A typical volumetric feeder [10]

In the mills, the solid fuel is pulverised and entrained by the pre-heated primary air stream to the burners [5]. The homogeneity of the fuel particle distribution between the burners fed by a given mill is generally checked during

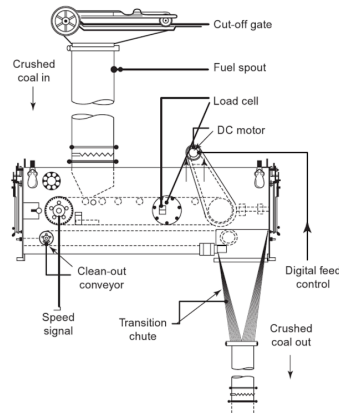


Figure 2: A typical gravimetric feeder [10]

commissioning, using manual flow rate measurements based on isokinetic sampling of the particles in the feed lines. Isokinetic sampling is illustrated in Fig. 3. In order to sample representative fuel particles, the gas velocity at the inlet  
 160 of the sampling orifice is controlled to be equal to the velocity of the local gas flow. When several points are covered in the section of a feed line, the total particle flow rate can be assessed. When the fuel flow rate is kept constant during the whole measurement procedure, this time-consuming technique can provide a reliable measurement of the particle flow rate for a given load. During  
 165 commissioning, the fuel flow rate balance between burners can be improved by modifying the relative pressure drops in the feed lines, through the adjustment of diaphragms. The obtained balance is however dependent on the type of fuel, the selected particle fineness and the load. Other parameters, like progressive coal particles deposition in the horizontal sections of the lines, can also im-  
 170 pact the fuel distribution. The homogeneity of the fuel distribution is rarely re-assessed during the lifetime of the boiler. Isokinetic sampling measurements can be carried out for trouble-shooting purposes.

It is here proposed to use microwave sensors to measure and monitor the fuel particle flow rates to the burners. This advanced, non-standard technique  
 175 is commercially available, and allows for a continuous monitoring of the fuel

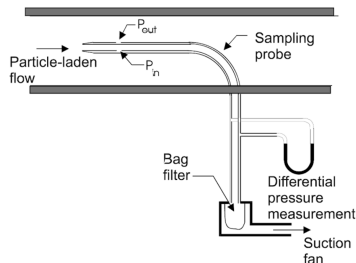


Figure 3: Principle of particle isokinetic sampling [11]

distribution to burners [3]. It is based on the detection of the microwaves reflected on the moving particles inside the pipes. The working principle of the EUcoalfow system developed by EUTECH is explained in details in [12] and is illustrated in Fig. 4. Unlike classical sampling techniques, this system provides  
 180 the detailed fuel-side data needed for an online control of the local AFR's. The detected signal is a linear function of the particle mass flow rate, but the absolute flow rate value is not directly measured. Relating these signals to the total coal mass flow rate pulverised in the mill, the collected data give an access to the individual mass flow rates sent to each burner. This is part of a calibration  
 185 procedure that needs to be carried out onsite, see §3.2. In order to cover the whole cross section, 2 to 3 sensors are installed per coal feed line. The estimated error in steady state phases (feeder flow rate vs. EUcoalfow total flow rate) is less than 4%. The precision (repeatability) of the measurements was assessed on a test bench, by quantifying the standard deviation of a series of measurements.  
 190 It was lower than 2% [5].

### 2.2. Air flow distribution to burners: soft sensors

As explained in § 1.4, not all boilers are equipped with air flow measurements per burner or burner row. And when they are, the accuracy of those measurements is typically lower than the total air flow rates measured at the  
 195 outlet of the forced draft fans. In order to get a detailed picture of the combustion air distribution in the furnace, and/or to challenge the existing local measurements, alternative model-based strategies can be used to compute the

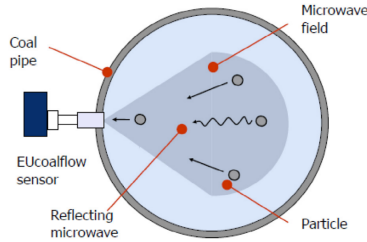


Figure 4: Working principle of the EUcoalflow microwave sensor [12]

local air flow rates [13, 14]. The basic principle of the proposed strategy is to take advantage of the most reliable physical measurements that are available to reconstruct the air flow distribution [3]. Typically, a model of the hydraulic network of the boiler is trained based on three types of data:

1. The local pressure measurements along the network;
2. The damper openings;
3. The reliable air flow measurements that are available (e.g. local and total air flow measurements, or excess  $O_2$  measurements).

Using this information, it is possible to determine the pressure drop characteristics of each portions of the air distribution system. Equivalent flow resistances  $\varphi_i$  are then determined, as illustrated in Fig. 5. Equation 3 gives the general relationship between a pressure drop  $\Delta p$ , the associated equivalent resistance  $\varphi_{eq}$  and the mass flow rate  $Q$ . Once the model is trained for a specific boiler, i.e. for the pipes, manifolds, dampers, fans etc. in their particular arrangement, it can compute the local air flow rates based on new, online data (e.g. fan load, pressures, damper openings, etc.).

$$\Delta p = \varphi_{eq} Q^n \quad (3)$$

The commercial EUSoft Air system based on this principle was used in this study [3]. Based on the industrial return of experience, significant discrepancies are often observed between the sum of the local measurements and the (more

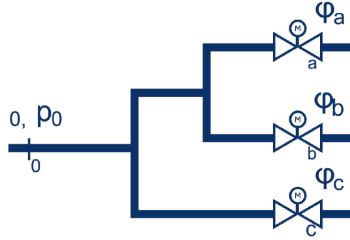


Figure 5: Working principle of the EUSoft Air soft sensors

reliable) total flow rates from the fans, which justifies the use of model-based approaches using simple and reliable data [3].

### 2.3. Air-Fuel ratio calculation

220 The use of advanced microwave sensors for the local fuel flow rates and soft sensors for the local air flow rates addresses the issues related to the standard equipment available on most commercial boilers for the calculation of local AFR's and  $\lambda$ 's. With those reliable data, the local AFR's per burner or burner row can be directly computed as per Eq. 1. As far as the local equivalence ratios  $\lambda$ 's are concerned, information on the fuel composition must also be taken into account to determine the stoichiometric amount of air needed to burn each kilogram of fuel ( $\dot{m}_{a,stoi}$ ) needed in Eq. 2. Reliable ultimate analysis of the fuel(s) is generally available to make that calculation, with however a larger uncertainty on the moisture content of the fuel. The fuel flow rate measured 230 by the feeders, and therefore by the microwave sensors, is indeed the total mass flow rate, moisture included. If the fuel has undergone partial drying or further humidification between the ultimate analysis and the injection in the boiler, the corresponding stoichiometric amount of air  $\dot{m}_{a,stoi}$  is modified. The other parameters of the ultimate analysis are not expected to change significantly during 235 storage.

The oxygen concentration in the flue gas can be used as a way to correct the initial moisture content of the fuel after calculation. From the AFR values, it is indeed straightforward to deduce the composition of the flue gases. The

following calculation procedure is therefore proposed:

- 240 1. Calculation of the stoichiometric amount of air per kilogram of fuel, based on the ultimate analysis of the fuel;
2. Measurement of the local fuel and air flow rates;
3. Calculation of local and global AFR's and  $\lambda$ 's using Eq. 1 and 2;
4. Calculation of the expected  $O_2$  content in the flue gases;
- 245 5. Comparison with the measured  $O_2$  concentration;
6. Correction of the fuel moisture content to match the measured  $O_2$  concentration;
7. Convergence towards the real local and global AFR's and  $\lambda$ 's.

If the discrepancy between the measured and the corrected moisture contents  
250 is high ( $> 10\%$ ), further investigation is needed to understand the possible causes for this evolution.

### 3. Case study

#### 3.1. Gheco-One power plant

The proposed methodology was applied to the coal-fired boiler of the 660  $MW_e$   
255 Gheco-One power plant, located in Thailand. The boiler is an opposed-fired, supercritical, pulverised-fuel boiler. It is depicted in Fig. 6.

Each one of the 6 mills (named A to F) feeds the 5 burners of a row. Above the 3 burner rows located on each side of the boiler, an additional row of OFA ports inject secondary air in the highest part of the furnace to complete the  
260 combustion process (air-staging as primary  $NO_x$  reduction measure). The arrangements of the burners and OFA ports on both Front and Rear Sides are illustrated in Fig. 7. The names of the mill feeding each row are indicated below the rows. In general, 5 mills are in service at full load operation (1 spare).

Two different types of coal were used during this study. The relevant composition parameters for the assessment of the stoichiometric quantities of air are  
265 summed up in Table 1. A corrected moisture content is also given. It will be

	Coal A	Coal B
C [% <i>m a.r.</i> ]	54.7	54.6
H [% <i>m a.r.</i> ]	3.92	4.14
N [% <i>m a.r.</i> ]	1.11	1.14
O [% <i>m a.r.</i> ]	12.11	13.07
S [% <i>m a.r.</i> ]	0.80	0.52
Ash [% <i>m a.r.</i> ]	4.76	4.52
Moisture [% <i>m a.r.</i> ]	22.63	22.05
Stoichiometric air flow [ <i>kg<sub>a</sub>/kg<sub>f</sub></i> ]	7.16	7.17
Corrected Moisture [% <i>m a.r.</i> ]	15.77	15.77
Corrected Stoi. air flow [ <i>kg<sub>a</sub>/kg<sub>f</sub></i> ]	7.77	7.77

Table 1: Coal compositions (as received) and corresponding stoichiometric amounts of air.

determined in §5, following the methodology proposed in §2.3. Coal A was fed to mills B, C and E, while Coal B was fed to mills A, D and F.

The primary air is fed to the 6 mills via dedicated lines, while secondary  
270 and Over Fired Air are distributed to wind-boxes, each of them covering one  
burners or OFA ports row, see Fig. 6. The wind-boxes are all fed from both  
the Left and Right Sides of the furnace, where the air flow rates are measured  
using multiports Pitot tubes and are controlled by dampers.

At the time of this study, the boiler exhibited a slight unbalance between  
275 Left and Right sides of the furnace regarding air flow rates, Furnace Exit Gas  
Temperature (FEGT), oxygen content in the flue gas and  $NO_x$  content in the  
flue gas. While it is supposed to be symmetric, the sum of the secondary air flow  
rates measured on each sides of the wind-boxes (Left and Right Sides) differed  
with  $\sim 20$  kg/s, for a total secondary air flow rate of  $\sim 560$  kg/s at full load.  
280 It was however unclear whether this discrepancy was physical, or the result of  
measurement errors at the inlet of the wind-boxes. A rule of thumb is that such  
an unbalance should remain lower than 2%, i.e.  $\sim 10$  kg/s in this case. The  
FEGT is estimated using 6 thermocouples installed at the outlet of the furnace,

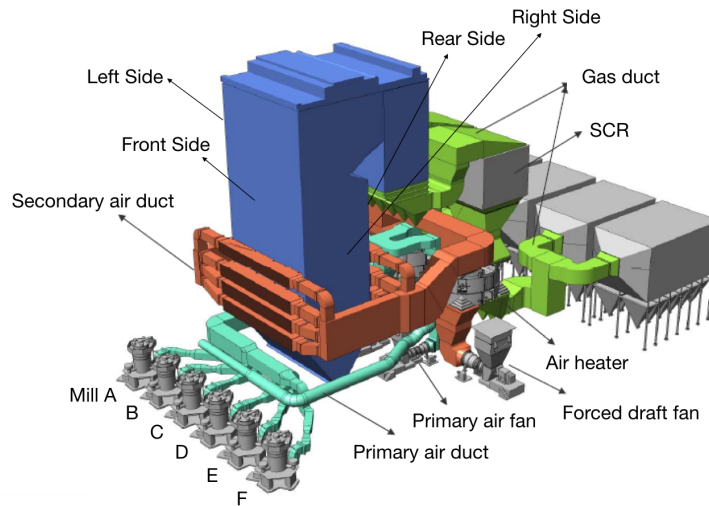


Figure 6: Pulverised-coal boiler of the Gheco-One power plant

close to the boiler wall (3 thermocouples on each side). A temperature difference  
 285 slightly higher than  $10^{\circ}\text{C}$  was observed, while it should ideally remain below  
 $10^{\circ}\text{C}$ . The  $\text{O}_2$  concentration measured by 6 paramagnetic devices (that had  
 been recently calibrated) located at the inlet of the De $\text{NO}_x$  Selective Catalytic  
 Reduction (SCR) system exhibited a discrepancy of more than 1% between  
 left and right. This value should ideally be kept under 0.5%. As far as  $\text{NO}_x$   
 290 concentrations are concerned, a difference of  $\sim 20$  ppm was observed between  
 the Left and the Right Sides, while a reasonable target would be  $< 10$  ppm. As  
 the SCR system is divided in two parallel trains (Left and Right), these slight  
 discrepancies were leading to a non-optimal operation of the De $\text{NO}_x$  system,  
 even if the emissions limit values were easily respected. A detailed analysis of  
 295 the fuel-air balance in the boiler was therefore carried out using the methodology  
 proposed here.

### 3.2. Materials and calibrations

The EUcoalflow microwave sensors were installed on all the coal feed lines.  
 The sensors were installed in straight horizontal sections, in a location suffi-  
 300 ciently away from upstream and downstream elbows ( $> 5$  m) to avoid the effect

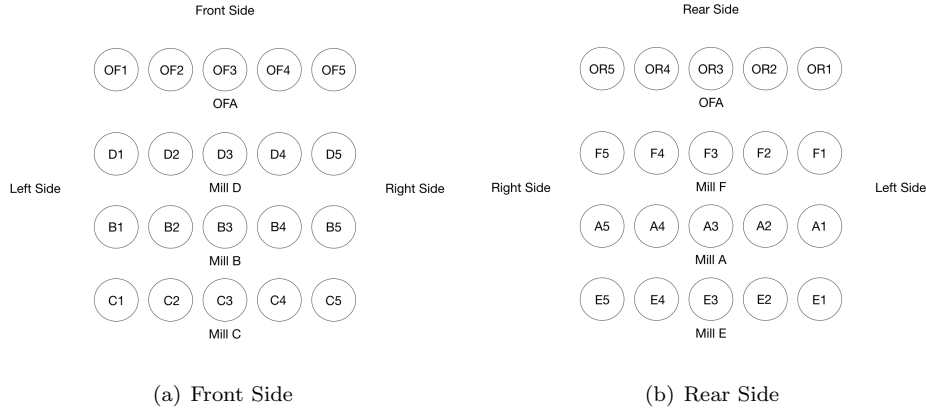


Figure 7: Burner arrangement on the Front and Rear Sides

of flow disturbance. For a complete coverage of the feed line sections, 3 sensors per line ( $3 \times 120^\circ$ ) were installed. The system was calibrated under steady state conditions: constant mill operations at various loads were used to deduce the linear relationship between the microwave signals and the coal flow rate in the feed pipes. Figure 8 illustrates the result of the calibration that was carried out onsite for coals A and B on Mills C and F, respectively. The linear relationship between the averaged mA signals retrieved from the microwave sensors and the feed line output flow rates in kg/s is such that the sum of the individual flow rates equals the total flow rate measured by the feeder. This relationship is dependent on the type of coal. The calibration results in an excellent agreement between the sum of the individual signals and the total flow rate measured by the feeder, for different loads. A short delay between the measurements is observed during the load transitions, due to the buffer effect of the mill itself.

The EUSoft Air soft sensors were trained using data retrieved from the plant Distributed Control System (DCS). The data was collected in the weeks preceding the test campaign, and after the latest outage of the power plant, in order to avoid any bias due to maintenance operations (sensor calibrations, damper mechanical adjustments,...). Figure 9 illustrates the validation of the soft sensors after their calibration, i.e. with another set of data than the one

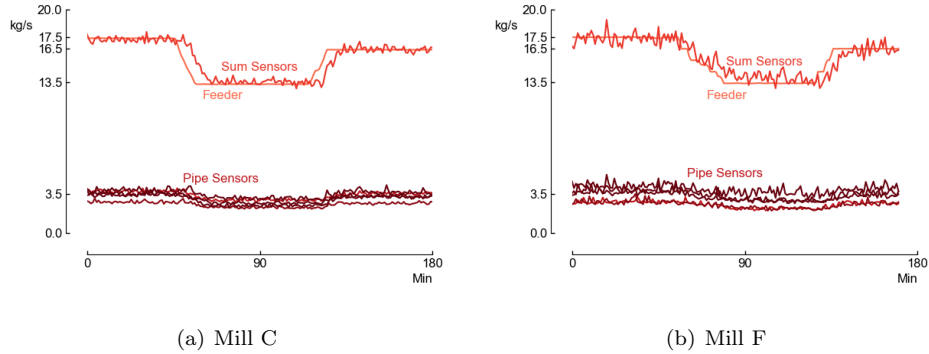


Figure 8: The sum of the calibrated microwave sensor signals is in excellent agreement with the feeder flow rates, for different loads.

320 used for calibration. It shows that the sum of the secondary air flows measured by the soft sensors is in much better agreement with the total FD fans flow than by the soft sensors is in much better agreement with the total FD fans flow than the sum of the local, physical measurements. It confirms that the combination of the pressure measurements and the damper openings with a model of the air distribution system can be more reliable than the local measurements. In this case, a discrepancy larger than 15% is observed between the FD fans and the local measurements. The small discrepancy between the FD fans and the soft sensors is due to the fact that the agreement with the total FD fan flow rates is targeted during a defined training phase, but not during subsequent uses of the model anymore. When new data is available, the trained model uses the pressure measurements and damper position to compute the local and total flow rates.

325

330

## 4. Results

### 4.1. Air flow measurements

The measurements performed with the calibrated soft sensors are continuous, and can be compared to the local, physical measurements. This comparison with the standard measurements is very useful to optimise the combustion process, as it allows to point out which flow rate measurements taken into account in

335

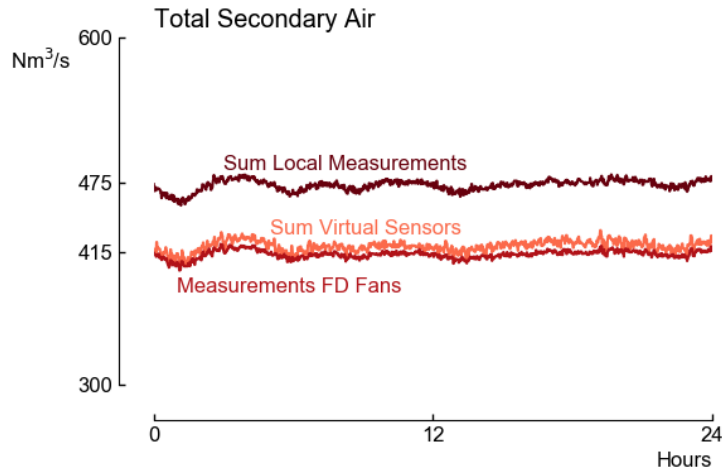


Figure 9: The sum of the secondary air flows measured by the soft sensors is in better agreement with the total FD fans flow than the sum of the physical measurements.

process control system might be a source of inaccuracy and/or unbalance. Figure 10 shows examples of both an agreement and a disagreement between the soft sensor and the physical measurement. As the soft sensor measurement are validated against the total FD fan flows, a disagreement is interpreted as an inaccuracy of the physical measurement.

The time-averaged air flow rates to the wind-boxes obtained during a 24 hours operation are shown in Fig. 11. They are compared to the corresponding physical measurements. Given the wind-box configuration of the studied air distribution system, it was assumed that the two left (resp. right) side burners of a wind box are equally fed by the left (resp. right) damper of the wind-box. Without further information about the static pressure at the inlet of each burner, it is indeed impossible to segregate between burners fed by the same side of a wind-box. The burners located in the center of the rows were supposed to receive half of their air flow rate from each side of the wind-box. In Fig. 11, the air flows are those measured for each mill when they are at full load (while the boiler generally operates with 5 mills in service and 1 spare mill). The global picture is therefore not representative for the general operation of

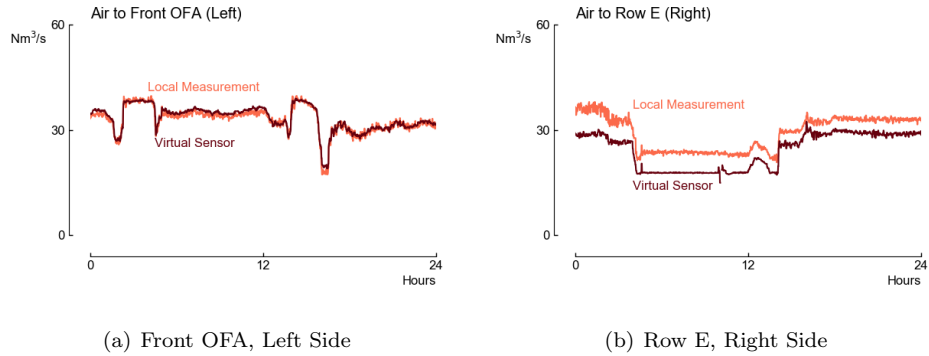


Figure 10: Comparison of physical measurements and virtual sensor measurements of local secondary air flows: agreement for the left side of the Front OFA wind-box, and significant discrepancy for the right side of the Row E wind-box.

355 the boiler, but for each burner row taken separately. For the OFA ports, the given values are those for a configuration where Mill F is out of service, which explains the lower air flow rate measured on the Rear Side OFA level compared to the Front Side.

As expected from the comparison of the total secondary air flows in Fig. 9, 360 the global trend is that the physical measurements overestimate the secondary air flows. While the Front Side OFA row shows a very good agreement between both measurements, the discrepancy on the Right Side reaches  $-24\%$ . Among the burner rows, the largest discrepancy is observed on the right side of the Mill E ( $-16\%$ ). For the other burner rows, the discrepancy is globally in the range 365  $5 - 10\%$ , which is within the expected accuracy of the measurement systems. However, the occurrence of a few larger discrepancies and the systematic overestimation of the flow rates by the physical measurements is problematic in terms of assessment of the local and global AFR's, as will be shown in §5. A random spread of virtual sensors measurements around the physical measurements 370 would have been less consequential.

Once potential sources for unbalances are identified using such a comparison, a tuning process can begin, during which the causes for the observed discrepancies between the measured and the real air flow rates are to be determined.

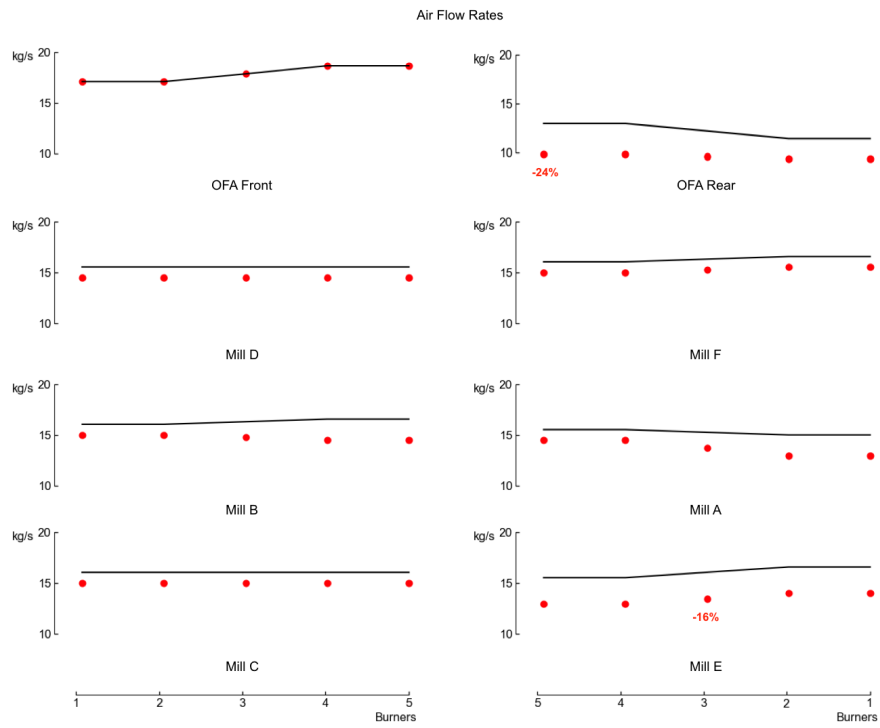


Figure 11: Individual air flow rates per burners: local measurements (lines) vs. virtual sensors (dots).

Those causes can be of different types:

- 375
- Uncorrected or wrongly corrected bias in the local flow rate measurement system;
  - Faulty treatment of the signal from the local transmitter in the DCS;
  - Physical bias in the position of a damper.

Each suspicious local measurement or actuator must be carefully checked.

380 Short term correction is not always possible on all the parameters. During this study performed on a boiler in continuous commercial operation, air flow rates unbalances were the only available lever to fine tune the combustion process. Coal flow unbalances were observed, see §4.2, but were not directly addressed.

Unbalance (Left-Right)	Good practice	Initial	Final
$\Delta$ Total secondary air [kg/s]	< 10	$\sim 20$	3 – 7
$\Delta$ FEGT [ $^{\circ}$ C]	< 10	$\sim 10$	2 – 7
$\Delta$ O <sub>2</sub> [% <sub>w</sub> ]	< 0.5	$\sim 1$	0.3 – 0.7
$\Delta$ primary NO <sub>x</sub> [ppm]	< 10	$\sim 20$	< 5

Table 2: Reduction of combustion unbalances achieved in this case study after investigation on suspicious secondary air flow rate measurements and/or control loops.

The Left-Right combustion unbalance mentioned in §3.1 was specifically ad-  
385 dressed. After the assessment of all the suspicious secondary air control loops,  
the initial unbalances were reduced in a significant extent, as summarised in  
Table 2. The given values are representative for the oscillation ranges observed  
during commercial operation.

#### 4.2. Coal flow measurements

390 Figure 12 shows the comparison between the expected coal flow rates per  
burners (one fifth of the feeder’s flow rate) and the flow rates measured with  
the microwave sensors. These values were measured for each mill when it was  
running at full load. As the boiler is generally operated with 5 mills at full load,  
Fig. 12 is therefore not representative for the general operation of the boiler,  
395 but for each burner row taken separately.

The maximum discrepancy is observed on burner B3 (–29%). Significant  
coal dust deposition in the horizontal sections of the corresponding feed line  
was suspected. Deviations around  $\sim 20\%$  are also found in rows C, E and F (7  
burners in total). For the other burners, the deviations remain in the acceptable  
400 range of  $\pm 15\%$ . Mill A exhibits an excellent agreement with the expected values  
(< 5%). While the air flow soft sensor measurements can disagree with the  
physical ones regarding the total flow rate, it cannot be the case for the coal  
flow rates, due to the calibrations of the system vs. the feeder flow rates, that are  
considered as reliable data. Hence, the detailed measurements are per definition  
405 evenly distributed around the expected values.

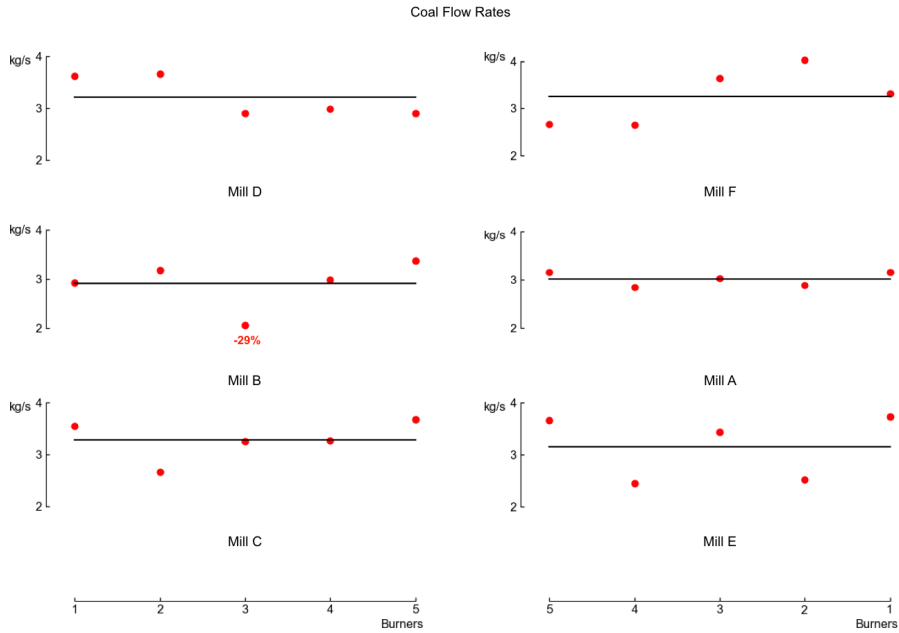


Figure 12: Individual coal flow rates per burners: expected values (lines) vs. measured values (dots).

## 5. Equivalence ratios

Using the air flow and coal flow measurements described in §4, it is now possible to compute the local equivalence ratios for all burners, and to compare it with the expected values deduced from the standard measurements available in the power plant. In order to do this, the available information on the coal  
 410 composition must also be used to determine the stoichiometric amount of air per kilogram of fuel, see 1. The results are illustrated in Fig. 13. As for the air and coal flow measurements, these results are valid for each mill running at full load, and are therefore not representative for the normal operation of the boiler  
 415 (1 spare mill, most often Mill F).

While the expected equivalence ratios are in the range 0.9 – 1.05, the measured values exhibit a significantly extended range: 0.7 – 1.36. The highest value clearly results from the decreased coal flow rate fed to burner B3, while

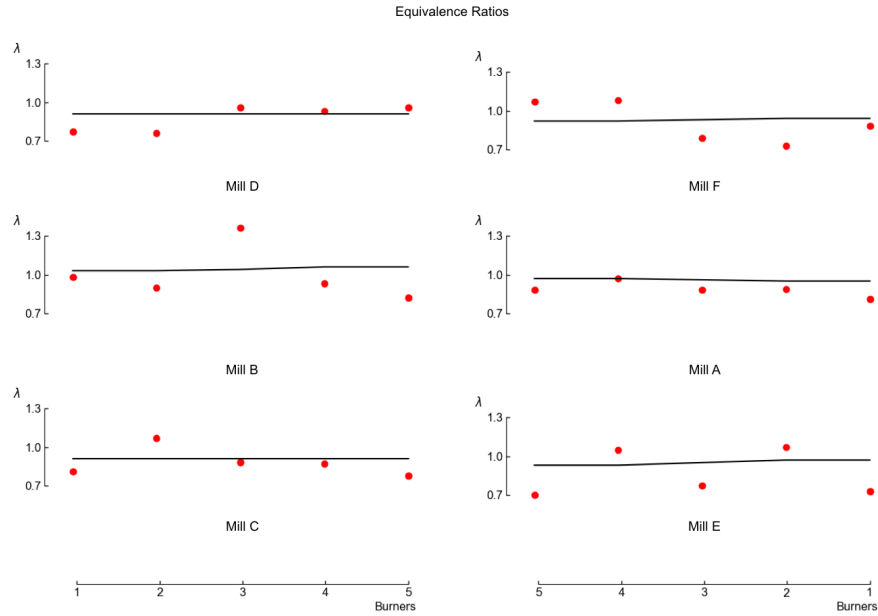


Figure 13: Individual equivalence ratios per burners: expected values (lines) vs. calculated values (dots).

the lowest value is due to the combination of a low total air flow rate and a poor  
 420 coal flow homogeneity for Mill E. The measured data are not evenly distributed  
 around the expected ones: they are shifted towards lower  $\lambda$ 's, due to the general  
 positive bias on the local air flow measurements.

The gathered information, combined with the available primary air flow rate  
 measurements, also allows for an assessment of the oxygen content in the flue gas  
 425 at the outlet of the furnace. For an operation mode with Mill F out of service,  
 an  $O_2$  concentration of 3.6% (humid) is predicted. However, the average  $O_2$   
 concentration measured during the campaign was 2.5% (humid). As proposed  
 in §2.3, the moisture content of the fuel was adapted in order to fit this value.  
 The results were given in Table 1. In order to match the measured oxygen, the  
 430 moisture contents must be reduced from 22.63 and 22.05 to 15.77%<sub>m</sub>, resulting  
 in stoichiometric air quantities corrected from 7.16 and 7.17 to 7.77 kg<sub>a</sub>/kg<sub>f</sub>.

The corrected equivalence ratios per burner are compared to the expected

ones in Fig. 14. The measured values now range between 0.65 (burner E5) and 1.25 (burner B3), and only 6 burners have higher equivalence ratios than expected.

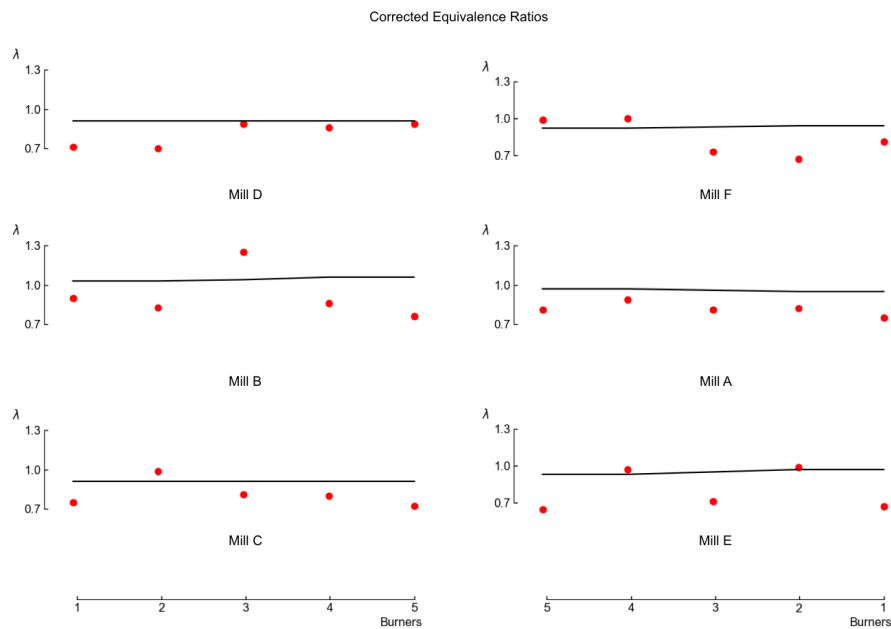


Figure 14: Corrected individual equivalence ratios per burners: expected values (lines) vs. calculated values (dots). Correction based on the measured  $O_2$  concentration in the flue gas.

Interesting for our analysis is the cumulative value of equivalence ratio along the height of the boiler. The local  $\lambda$ 's were added per level and cumulated to give an image of the segregation between the reducing and oxidising zones of the furnace. The result is shown in Fig. 15. The 'expected' scenario was built using the local secondary air measurements. Using the total flow from the FD fans to compute the final value of  $\lambda$  would result in the same value as the 'measured' scenario, as the soft sensors measurements are in agreement with the total flow from the fans.

While the standard equipment available on the boiler predicts a switch from reducing to oxidising atmosphere at the level of Mills D and F, the measured and corrected values indicates that the stoichiometric conditions are only reached

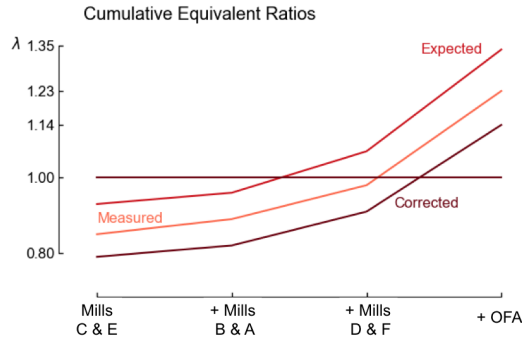


Figure 15: Cumulated equivalent ratios along the height of the furnace.

at the OFA level, which significantly increases the volume of the furnace that is subject to a substoichiometric composition of the flue gases. The final value of  $\lambda$  that is in agreement with the measured  $O_2$  content in the flue gas is of course 1.14 (corrected measurements). Also, while it is a priori expected that the lowest value of  $\lambda$  is 0.93 (bottom of the furnace), it appears that the lowest measured and corrected values are 0.85 and 0.79 respectively.

The targeted values of  $\lambda$  in the furnace are dependant on the type of burners and the chosen primary  $NO_x$  emission reduction measures. As explained in §1.2, low- $NO_x$  burners can be combined with global air-staging for optimal performances, in which case the burner  $\lambda$  can be lower than unity, even for modern burners. In order to reduce the drawbacks related to reducing atmospheres in the combustion zone (see §1.2), it is however generally considered that local equivalence ratios lower than 0.8 should be avoided. This study shows that the considered boiler is actually running at a relatively low  $\lambda$  for the lowest burner rows.

## 6. Conclusions

In this study, a novel methodology was proposed to monitor the air-fuel and equivalence ratios at the level of the burners in large pulverised-fuel boilers. It is based on the combination of advanced (though commercially available) mea-

surement systems: microwave sensors for the distribution of coal among the burners fed by the same pulveriser, and soft sensors for the distribution of combustion air. Both those systems complete or challenge the standard equipments usually available, and can be used separately for trouble-shooting or fine tuning  
470 purposes.

When combined, they offer a straightforward assessment of the local air-fuel ratios. When the composition of the fuel is known, local equivalence ratios can also be calculated. It was however shown that the uncertainty on the fuel moisture content can significantly impact the results. Matching the measured  
475 oxygen content in the flue gas was therefore proposed as a mean to correct the measured values.

The proposed methodology was successfully applied to the boiler of a  $660\text{MW}_e$  coal-fired power plant. The performed air flow measurements alone were used to tune the combustion process by solving hardware and software issues. Oxygen,  
480 flue gas flow rate, temperature and  $\text{NO}_x$  unbalances at the outlet of the furnace were significantly reduced. Both advanced coal and air flow measurements were combined to compute local equivalence ratios. While the burner equivalence ratios predicted by the standard equipments were in the range  $0.9 - 1.05$ , it was shown that the actual range was significantly broader ( $0.65 - 1.25$ ). Looking at  
485 the averaged ratios per burner level, it was concluded that the expected values were globally overestimated compared to the measured values ( $> +14\%$ ). The burner level at which the combustion becomes globally stoichiometric is also underestimated. As a consequence, the volume of the furnace that is submitted to a reducing atmosphere is significantly larger than expected, increasing the  
490 risks for corrosion or slagging issues.

The proposed methodology was proved useful to assess the local air-fuel ratios in a large pulverised-fuel boilers. The gathered information is crucial to perform a relevant analysis of the air and fuel distribution in the burners, and to optimise the combustion process while keeping the primary pollutant emissions  
495 to an acceptable level.

## References

- [1] IEA, Key world energy statistics, Tech. rep., International Energy Agency, Paris (2016).
- [2] European Commission, Best available techniques (BAT) reference document for large combustion plants (draft), Tech. rep., Institute for Prospective Technological Studies (2016).  
500
- [3] M. Wiatros-Motyka, Optimising fuel flow in pulverised coal and biomass-fired boilers, Tech. rep., IEA Clean Coal Centre (2016).
- [4] H. Spliethoff, Power Generation from Solid Fuels, Springer, London, 2010.
- [5] J. Blondeau, R. Kock, J. Mertens, A. Eley, L. Holub, Online monitoring of coal particle size and flow distribution in coal-fired power plants: Dynamic effects of a varying mill classifier speed, Applied Thermal Engineering 98 (5) (2016) 449–454.  
505
- [6] G. Lai, High-Temperature Corrosion and Materials Applications, ASM International, 2007.  
510
- [7] G. Couch, Understanding slagging and fouling in pf combustion, IEA Coal Research, 1994.
- [8] R. Bryers, Fireside slagging, fouling, and high-temperature corrosion of heat-transfer surface due to impurities in steam-raising fuels, Progress in Energy and Combustion Science 22 (120) (1996) 29.  
515
- [9] R. Baker, Flow Measurement Handbook, Cambridge University Press, 2000.
- [10] D. Sarkar, Thermal Power Plant: Design and Operation, Elsevier, 2015.
- [11] C. Crowe, J. Schwarzkopf, M. Sommerfeld, Y. Tsuji, Multiphase Flows with Droplets and Particles, Taylor and Francis Group, 2012.  
520

- [12] M. Starke, R. Kock, M. Haug, M. Schreiber, F. Turoni, Continuous measurement of coal flow and air-fuel ratio inside coal pipes for closed-loop control, Power Gen Europe Conference 2010.
- [13] F. Turoni, A. Hawenka, C. Lindscheid, M. Haug, M. Schreiber, Optimizing combustion using state-of-the-art model predictive control strategies, in: International Conference on Thermal Power and Sustainable Development (TENOR 2011), 2011.
- [14] E. Martensen, A. Heyer, M. Sikira, A. Camdzic, Kostenoptimierte minderung von hochtemperaturkorrosion am beispiel eines kohlebefeueren 230 mw blocks, in: Kftwerkstechnisches kolloquium 2016.